Available online at www.sciencedirect.com

ScienceDirect

Chinese Journal of Aeronautics 22(2009) 145-152

Chinese Journal of Aeronautics

www.elsevier.com/locate/cja

Conjugate Calculation of Gas Turbine Vanes Cooled with Leading Edge Films

Dong Ping*, Wang Qiang, Guo Zhaoyuan, Huang Hongyan, Feng Guotai

School of Energy Science and Engineering, Harbin Institute of Technology, Harbin 150001, China

Received 25 February 2008; accepted 20 May 2008

Abstract

Conjugate calculation methodology is used to simulate the C3X gas turbine vanes cooled with leading edge films of "showerhead" type. By comparing calculated results of different turbulence models with the measured data, it is clear that calculation with the transition model can better simulate the flow and heat transfer in the boundary layers with leading edge film cooling. In the laminar boundary layers, on the upstream suction side, the film cooling flow presents 3D turbulent characteristics before transition, which quickly disappear on the downstream suction side owing to its intensified mixing with hot gas boundary layer after transition. On the pressure side, the film cooling flow retains the 3D turbulent characteristics all the time because the local boundary layers' consistent laminar flow retains a smooth mixing of the cooling flow and the hot gas. The temperature gradients formed between the cooled metallic vane and the hot gas can improve the stability of the boundary layer flow because the gradients possess a self stable convective structure.

Keywords: gas turbine; conjugate calculation; leading edge film cooling; transition; temperature gradient

1. Introduction

To raise the thrust-to-weight ratio and thermal efficiency of a gas turbine engine, hot gas temperature is often required to break the limits stipulated by the turbine blade and vane blade materials. The challenges the gas turbine designers must face are not only to effectively shield the engine's critical components from the hottest gas, but also to precisely predict thermal loads of the cooled components with an ad hoc system, to support the stress-load analysis that ultimately determines their life.

The first stage of a high-pressure turbine of an aeroengine is submitted to very strong hot impingements. In practice, the showerhead film cooling technique, in which a number of separate rows of holes are disposed to emit a huge amount of air, to form homogeneous film coverage over the vane surfaces, is usually employed on the leading edges of the first stage of turbine guide vanes to shield the hot gas effectively. The mixing of the cooling film and hot gas is a very complex 3D flow and exerts a great influence on the external convection of turbine vanes in the boundary layers. Usually, measuring heat transfer on vane surfaces under operating conditions experimentally seems extremely expensive for industrial designing uses, therefore, typically, multiple iterations and decouple methods associated with empirically derived correlations are often adopted, although this strategy is sometimes too inaccurate to befit real services. Further development of modern numerical tools capable of accurately simulating the flow and heat transfer is urgently required for improving the advanced film cooling techniques and predicting the turbine vane lifespan. Since the 1990s, with advances in computational fluid dynamics (CFD) technology, conjugate heat transfer methodology for turbomachinery has become ripe and popular, thanks to its high efficiency and accuracy.

Being pioneers to introduce conjugate calculation technique (CCT) to numerical simulation of turbomachinery, D. Bohn, et al.[1] used the Glenn-HT code to calculate conjugate heat transfer on Mark II and C3X gas turbine guide vanes, which were cooled by a radial air flow through ten cooling holes, which L. D. Hylton, et al.[2] had used for their experiments. The results proved to be in good agreement with those from the experiments. D. W. William, et al.[3] performed another CCT simulation of C3X vanes with commercial CFD codes Fluent 5, and B. Facchini[4]

*Corresponding author. Tel.: +86-451-86412433.
E-mail address: dps777@163.com
Foundation item: National Natural Science Foundation of China (50476028, 50576017)

doi: 10.1016/S1000-9361(08)60080-1

implemented Star-CD codes on the same vanes, but there were more errors in the results of their thermal dynamics calculation than in D. Bohn's. This could be blamed for the then commercial CFD codes being unable to make enough accurate simulation of the complex flow in the boundary layers. P. Dong, et al.[5] conducted a complete CCT analysis of Mark II vanes with commercial codes CFX 10 associated with a new transition model. The calculated temperature and heat transfer coefficient distribution accorded well with the measurements, and the results showed that the transition brought strong influences upon the flow conditions and heat transfer in the boundary layers of Mark II turbine guide vanes. Using the same Glenn-HT code, D. Bohn, et al.[6-8] extended the conjugated approach to investigate leading edge film cooling of the first stage rotor blades designed by KHI Ltd. The cooling configuration consisted of three rows of radial inclined holes with three serpentine internal passages. The calculated results agreed with the thermal paint measurements. J. D. Heidmann, et al.[9] upgraded the Glenn-HT code using the boundary element method (BEM) to calculate real film cooled turbine vanes, but left behind a deficiency in default of being compared to experimental data. BEM could cut down computational work because it did not require meshing of the solid domain.

For the purpose of investigating the mixing behavior and heat transfer between cooling film and hot gas in the boundary layers, this article carries out a 3D CCT simulation of a C3X high pressure nozzle guide vane with showerhead leading to edge film cooling. The computation model for numerical simulation is built based on the experimental study of E. R. Turner, et al.[10] in NASA, for Turner's work is well-known in the published heat transfer reference for that contains full information about the data measured from metal vanes, showerhead film cooling, and internal cool convection, under near realistic engine operating conditions.

2. Computation Scheme

C3X vane designed by Allision Ltd. has a constant cross-section and no twist. Fig.1 shows a view of cascade geometry and the computation mesh. Conforming with E. R. Turner's experiment[10], the vane was made up of two thermally isolated parts: the leading edge region and the test vane only serving to supply film cooling without being subjected to heat transfer measurements, and the former was neglected. In contrast, for both heat transfer and aerodynamic measurements, the latter was treated as the adiabatic region in the present computation.

The present computation employs periodicity conditions to replicate the multiple vane passages in the experiment, and only one vane is included in the 3D computational domain. The configuration of showerhead leading film cooling consists of five equi-spaced rows of holes, labeled as "C1", " C2", "C3", "C4"and "C5" in Fig.1, with the center row (C1) located near the stagnation point. Each row is arranged with ten or nine inclined holes, which are staggered radially midway between those in the adjacent rows. Every hole diameter d is 0.99 mm, with a radial inclined angle of 45°, a hole spacing of 7.5d, and a row pitch of 4.0d. There are ten radial flow cooling holes in the blade to supply internal cooling convection.

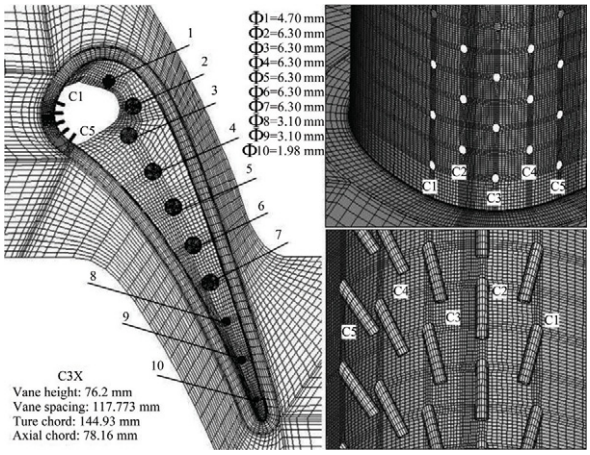

Fig.1 A view of cascade geometry and computation mesh.

A structured multi-block grid is used to decrease the number of cells in the present work. There are 1.84 million computation grids with about 65% in leading film cooling holes and boundary layers, 19% in passages, 5% in blades, and 11% in ten radial cooling holes. There are at least twenty points in the fluid boundary layers, and the first points from solid wall are located at the place where the dimensionless wall distance y^+ is less than or equal to unity for correct resolution of the viscous sublayer.

No.4313 operating conditions adopted by E. R. Turner, et al.[10] are simulated in present article. Table 1 lists the boundary conditions of the passages.

Table 1 Boundary conditions

Parameter	Value
Inlet total pressure/Pa	207 332.65
Inlet total temperature/K	690
Inlet turbulence intensity	6.5
Inlet viscosity ratio	10
Inlet Reynolds number	3.8×10^5
Outlet static pressure/Pa	127 510.03
Outlet Mach number	0.89
Leading edge film cooling flow mate/(kg·s^{-1})	0.001 71
Leading edge film cooling temperature/K	517.5
Radial cooling temperature/K	300

This calculation obeys laws for compressible ideal gas. The constant pressure specific heat (C_p) is denoted by a polynomial as a function of static temperature (T):

$$C_p(T) = 957.110\,256 + 0.236\,523\,4\,T + (5.141\,114\times10^{-6})\,T^2 - (3.391\,744\,6\times10^{-9})\,T^3 - (6.092\,964\,6\times10^{-12})\,T^4 \quad (1)$$

Dynamic viscosity (μ) and thermal conductivity (λ) of gas are taken from Sutherland's law and represented as a function of temperature.

$$\mu(T) = \mu_0\left(\frac{T}{T_0}\right)^{3/2}\frac{T_0+S}{T+S} \quad (2)$$

$$\lambda(T) = \lambda_0\left(\frac{T}{T_0}\right)^{3/2}\frac{T_0+S}{T+S} \quad (3)$$

where $\mu_0 = 1.789\,4\times10^{-5}$ Pa·s, $T_0 = 273.11$ K, $\lambda_0 = 0.026\,1$ W/(m·K), $S = 110.56$.

The material for the vane is of the ASTM type 310 stainless steel (0Cr25Ni20). From Ref.[11], this metal has a density of $\rho = 8\,030$ kg/m^3, constant pressure specific heat of $C_p = 502$ J/kg·K, and the thermal conductivity is specified to vary linearly with temperature, i.e.

$$\lambda(T) = 0.011\,5\,T + 9.910\,5 \quad (4)$$

With the intention of investigating the numerical errors in boundary layer flow simulation, this article chooses different turbulence models for calculation and comparison (see Table 2) including the γ transition model modified by F. R. Menter, et al.[12-13]. The present simulation uses commercial code CFX 10 and is conducted on a Dawning 2000 parallel computer, and the scheme of discretization is of second-order upwind accuracy.

Table 2 Turbulence models

Case	Model
Coupled case with leading edge film cooling	Standard k-ε model
	Renormalization group (RNG) k-ε model
	Standard k-ω model
	Shear-stress transport (SST) k-ω model
	SST k-ω model + γ transition model
Coupled case without leading edge film cooling	SST k-ω model + γ transition model
Adiabatic wall (without metal vane) with leading edge film cooling	SST k-ω model + γ transition model

3. Presentation of Results

3.1. Comparison with different turbulence models

Restricted by the previous test instrumentation and measuring methods, measurements[10] were only made on 2D aerodynamic, and heat transfer at midspan outer vane surfaces. Because of the radial inclination of cooling holes, there should be a significant radial flow component in the cooling flow, and the flow near the midsection region should be influenced by the 3D film cooling coverage on the vane surfaces. Therefore, if the 2D calculated variables at midspan extracted from the present 3D numerical simulation agreed with the measurement, it stood to reason that the calculation was correct for simulating the complex flow, with leading edge film cooling.

According to the boundary conditions listed in Table 1, the flow in the passages belongs to the midturbulence flow. Fig.2 shows that the calculated flow is subsonic; the main stream is accelerated to maximal Ma= 0.99, resulting in a shock at 40%-50% axial chord length on the suction side, and a weak shock just in front of the tailing edge. In Figs.3-5, the aerodynamic and heat transfer variables are in general dimensionless numbers. Z represents Z axial chord, $p_{\mathrm{tot,in}}$ the inlet total pressure, and L the axial chord length.

From Fig.3, it can be understood that, by comparing the pressure distribution along the vane wall with the experimental data, and the calculation with different turbulence models at the midspan of vane height, quite

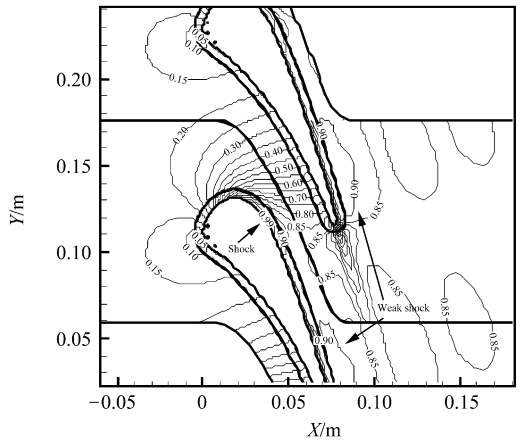

Fig.2 Predicted Mach number distribution at midspan.

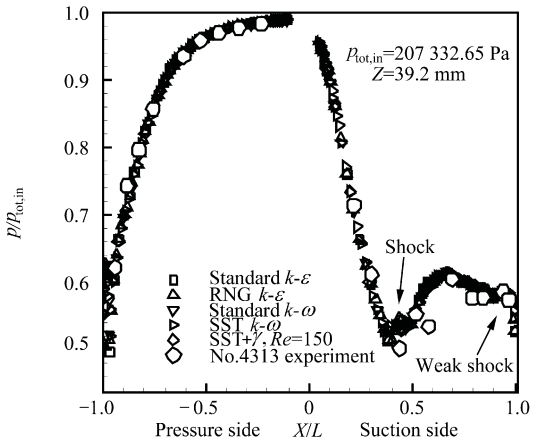

Fig.3 Predicted and measured aerodynamic loading distribution on vane external wall at midspan.

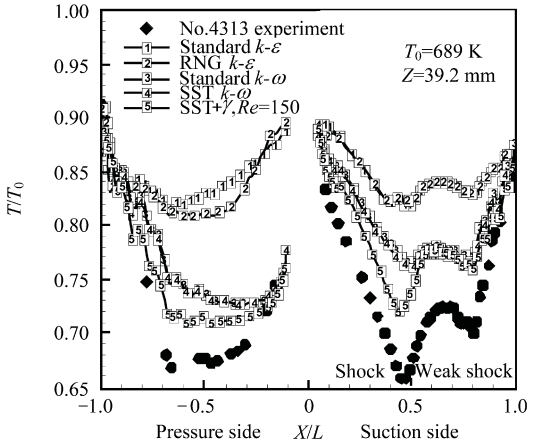

Fig.4 Predicted and measured temperature distribution on vane external wall at midspan.

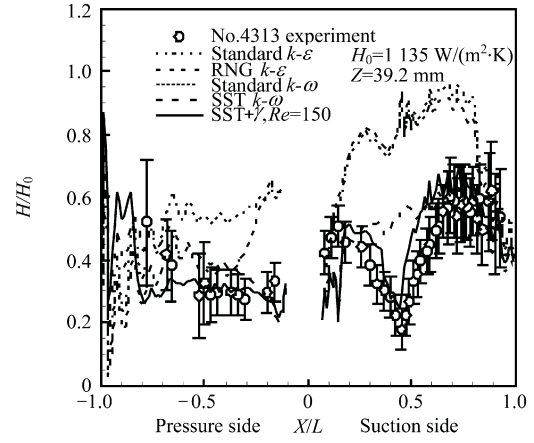

Fig.5 Predicted and measured HTC distribution on vane external wall at midspan.

a good agreement between them is achieved. The pressure distribution indicates that the analog of the main stream fields is computed with different turbulence models owing to the zero static pressure gradients in the boundary layers. Also in Fig.3, at the position where the strong shock occurs, a severe downstream pressure fluctuation with sharp increases and decreases in the pressure can be seen, and the corresponding flow is decelerated and accelerated again to the second weak shock. This gradient is usually thought to induce transition flow.

The commonly acceptable critical Reynolds number for transition equals 3.5×10^5, and the chord length Reynold number of a typical gas turbine ranges from 1×10^5 to 1×10^7, which means transition would most probably occur under typical gas turbine operating conditions. Transition has a remarkable influence on losses and heat transfer in turbine passages because the flow regions before and after transition have distinct velocity profiles and shear stresses. It is clear from Fig.4 and Fig.5 that calculation with the transition model results in curve whose shape is identical to that of the measurements, and the error among all turbulence models appear the smallest. The maximum difference in temperatures between the calculation with γ transition model and the measured results is equal to or less than 5%, and the maximum discrepancy of heat transfer coefficients (HTC) between them is about 10%. From Fig.4 and Fig.5, it is evident that only calculation with the transition model can clarify the sharp reverse after the strong shock at the position of 45% axial chord length. Therefore, it is conceivable that the transition flow surely occurs in C3X passages and produces enormous effects on heat transfer in boundary flow.

There are two factors that are thought to aggravate the accuracy of the calculation, without using transition models: ①the dual-equation turbulence models used in this article are all based on the Boussinesq hypothesis which adopts the Reynolds averaged approach and some empirically derived correlations. ②these models usually ignore the influences of transition by regarding the whole boundary layer field as a full turbulence flow. The calculation with the k-ε turbulence model (standard and RNG) has the largest discrepancy because it adopts the wall function method, to simplify the flow in the boundary layers with semi-empirical formulas. In contrast, the calculation with the k-ω turbulence model (standard and SST) has a smaller discrepancy, but it adopts empirical damping functions to simulate the viscous effects in boundary layers, which may not accurately tell the transition flow apart. Therefore, out of the urgent need for an effective transition model to precisely simulate the boundary layer flow, the transition model used in this article has been amended by F. R. Menter, et al.[12], and proves to be useful for the calculation of boundary layer cases[13].

3.2. Film cooling flow in boundary layers

The flat plane shown in Figs.6-9 is a spread vane surface from the leading edge stagnation point to the tailing edge along the blade profile. In Figs.8-9, the film cooling temperature iso-line map in the leading edge is used to demonstrate the cool contrail for downstream flow in default of the calculated HTC data on the adiabatic region. Figs.6-9 also show the approximate position where the strong shock occurs and in Figs.2-5 the 2D data extraction line which is intersected by the vane surface at Z = 39.2 mm can be seen.

Fig.6 illustrates a detailed uncoupled film cooling temperature distribution on the adiabatic vane wall. The low temperature contrails show the effective coverage of film cooling: the suction side is covered by ejections from rows C1 and C2, and the pressure surface from rows C3, C4, and C5. These contrails also show a significant radial flow component in the cooling flow around the leading edge region because of the radial inclined angle of film holes. The temperature of the film cooling contrails gradually increases from the leading edge to the tailing edge because of its mixing with hot gas. It is noted that the wide leading edge

region between rows C2 and C3 on the suction side remains unprotected. Unlike other ejections that are reattached to the boundary rapidly by the push of the main stream, ejections from the C3 row thrust the local thin boundary layer and reattach on the downstream pressure side, farther because the C3 row is located near the stagnation point of the leading edge, where the local velocity of the free stream is decreased to zero, which finally results in a deteriorating cooling efficiency in the backward region of the C3 row compared to the similar region of the other cooling holes. From Fig.6, it is noticeable that the data extraction line at $Z = 39.2$ mm is located between two neighbor film cooling contrails on the pressure side, and the line lies just under the film cooling contrail on the suction side. T_w is wall temperature.

Fig.7 shows the temperature distribution under a coupled condition. There is a rapid decrease in surface temperature on the suction and pressure sides in contrast to the adiabatic wall case, and the film cooling contrails will soon turn obscure on the downstream coupled vane surfaces too. This may be ascribed to the large thermal conductivity of metal and the ten radial cooling channels, which render the heat transfer on vane surfaces higher than the leading edge film cooling.

In Fig.8, it is obvious that HTC distribution looks very inhomogeneous in the coupled case, and the regions under film cooling coverage displaying HTC lower than the space between the film cooling contrails. H_{fc} is heat transfer coefficient with film cooling.

In contrast with the same region near the data extraction line ($Z = 39.2$ mm) in Fig.7 and Fig.8, it is conceived that the film cooling contrail exerts more influences on the HTC distribution than on temperature distribution. The main function of film cooling is not to cool the vane directly but to separate hot gas from the vane wall and reduce the heat transfer from the hot gas into vane wall.

Fig.9 shows the ratio of HTC with the leading edge film cooling to that without film cooling on the vane wall under the coupled condition. Although in Fig.9 the ratio in the film cooling region is lowered significantly, the HTC ratio in the area between the film cooling contrails approaches unity, which means that, in this area, HTC with leading edge film cooling nearly equals the HTC without it, and it fails to provide effective protection for the area between film cooling contrails. This induces the need for another cooling method to improve the cooling efficiency of the downstream vane wall. H_{nfc} is heat transfer coefficient with nonfilm cooling.

As a dimensionless number to describe the flow characteristics of boundary layers, the shape factor of boundary layers is expressed by $H=\delta_1/\delta_2$, where δ_1 is the displacement thickness of a boundary layer and δ_2 its momentum thickness. The shape factor of a laminar

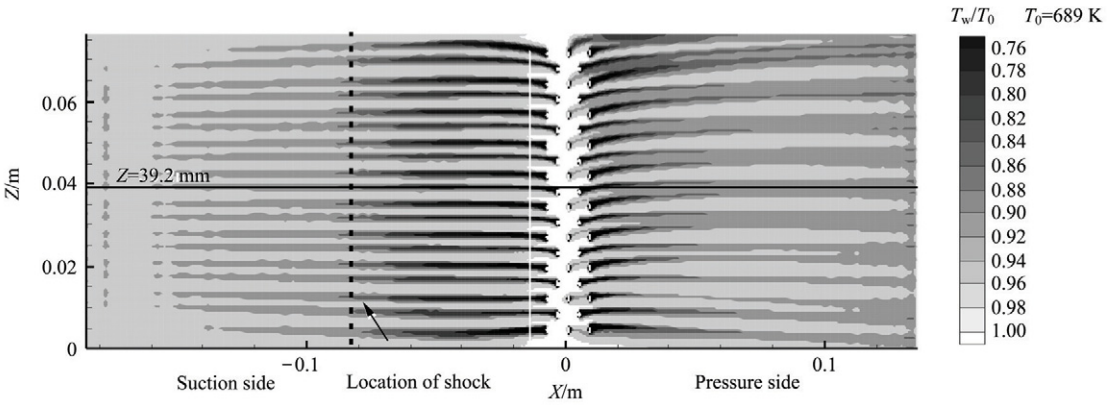

Fig.6 Predicted temperature distribution for uncoupled case with leading edge film cooling.

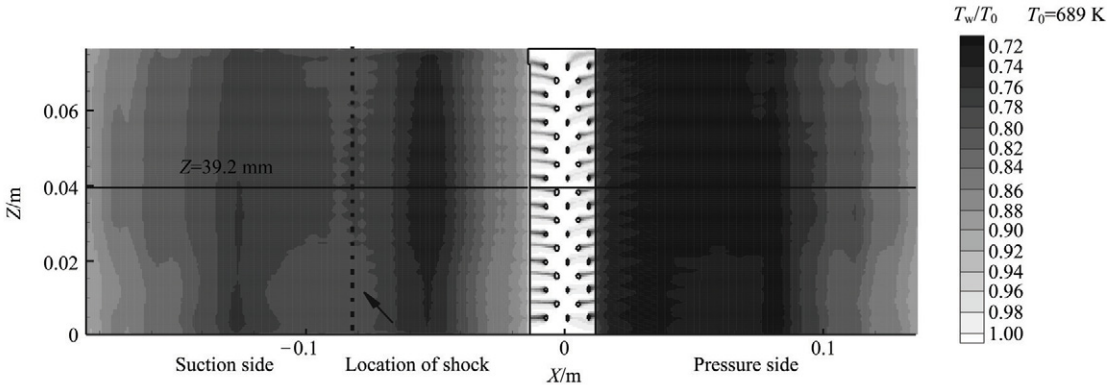

Fig.7 Predicted temperature distribution for coupled case with leading edge film cooling.

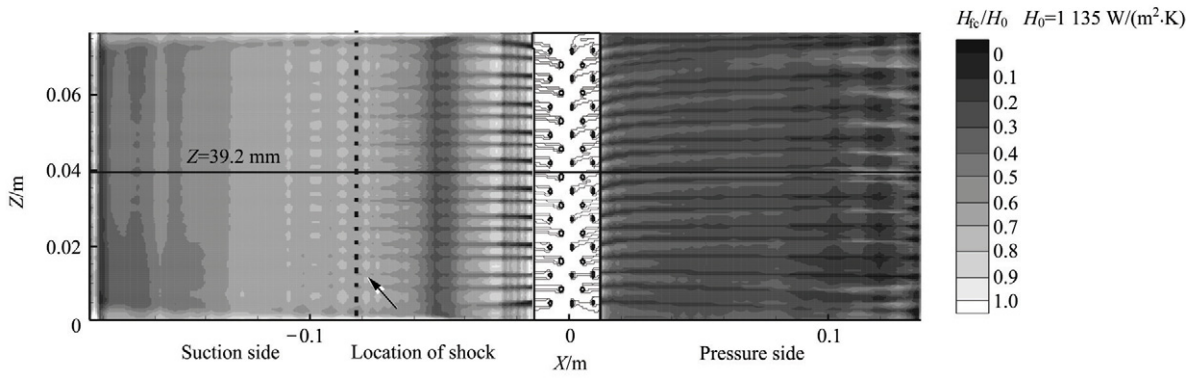

Fig.8 Predicted HTC distribution for coupled case with leading edge film cooling.

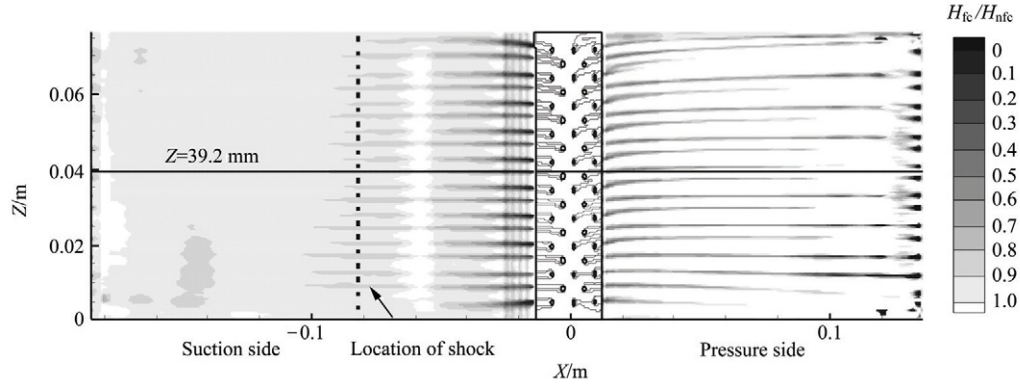

Fig.9 HTC ratio distribution for coupled cases.

boundary is more than 2.0, whereas, the one of a turbulent boundary equals or is less than 1.5. If a transition flow occurs in boundary layers, the shape factor must undergo a skip from 2.0 to 1.5. To investigate the boundary layer flow with and without leading edge film cooling, as well as, the influences of temperature gradient upon film cooling in boundary layers, Fig.10 compares three modes of shape factor distribution under various conditions inclusive of: on sections normal to the vane wall, under coupled conditions with and without leading edge film cooling, and in the adiabatic case (without metal vane) with leading edge film cooling. Under the coupled condition without leading edge film cooling, the boundary layer flow on sections 1-8 is of a laminar type with $H \approx 2.0$, then transition flow occurs on the suction sections 9-10, finally changes into the turbulent type with $H \approx 1.5$ on the suction sections 11-17, but remains laminar on all pressure sections. Under the coupled condition with leading edge film cooling, the shape factor curve severely fluctuates on the suction sections 1-8, with the shape factor of its crest representative of the area between the film cooling ejections equal to that of the mainstream boundary layers without film cooling ($H \approx 2.0$), and the trough of shape factor curve ($H \approx 1.5$) representing turbulent film cooling ejections. The fluctuation evidences that the film cooling ejection retains its distinct 3D turbulent flow characteristics, by lack of thorough mixing with the laminar mainstream, on the suction walls before transition. However, after the mainstream boundary layers have turned into turbulent flow on the suction sections 9-10, the fluctuation of the shape factor curve gradually becomes smooth and finally disappears on the tailing edge, because the mixing of hot gas and film cooling ejections is intensified by the turbulent flow in the boundary layers with the film cooling ejection being rapidly absorbed by the mainstream and losing its 3D flow characteristics. It can also be seen from Fig.8 that the lower HTC caused by the film cooling contrails disappears rapidly after the location of shock on the suction side for the same reason. Unlike on the suction side, the shape factor curve keeps on fluctuating on the pressure side sections 1-8, in other words, the film cooling ejections remain turbulent on the whole pressure side because the transition does not occur in the mainstream boundary layers, and the film cooling flow keeps its distinct 3D turbulent flow characteristics similar to the flow on the suction side before transition.

It is worthwhile to pay more attention to Fig.10, where it can be seen that the temperature gradients influence the film cooling flow to some extent in the boundary layers. In the uncoupled case without metal vanes, the adiabatic boundary layer has no temperature gradients and works in a manner opposite to the coupled case. In Fig.10, the shape factor under the coupled condition with leading edge film cooling is slightly higher than under the uncoupled condition for the reason that the temperature gradients caused by the temperature difference in metal vanes has a self-stable

convective structure, and can slightly delay the occurrence of transition in the boundary layers[14], therefore, the shape factor will most probably be influenced by the change of flow condition.

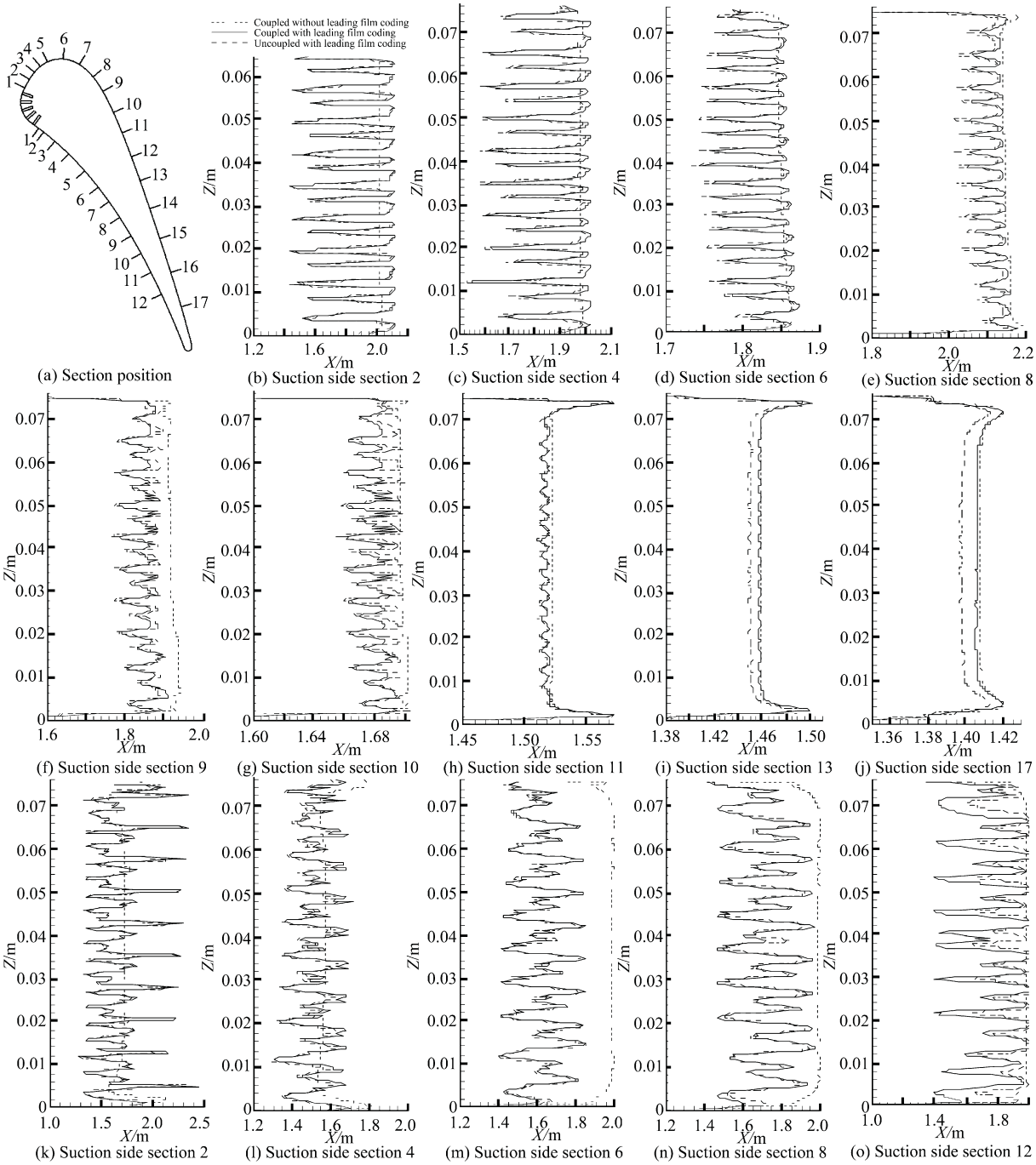

Fig.10 Shape factor on section normal to vane surface.

4. Conclusions

This article aims to use the conjugate calculation methodology to simulate the C3X gas turbine vane with "showerhead" type leading edge film cooling. The results demonstrate that application of transition model in calculation can more accurately predict complex mixing flow between mainstream and film cooling ejections in the boundary layers than in other turbulence models. The film cooling flow presents 3D turbulent characteristics in the boundary layers and the transition flow exerts significant influences on the flow and heat transfer characteristics on the vane surfaces. The temperature gradients caused by the difference between the cooled metal vane and hot gas can improve the stability of the boundary layer flow because it has a self-stable convective structure, which is able to delay the occurrence of transition in the boundary layers. The analysis of the conjugated heat transfer simulation of gas turbine vanes proves the accuracy

and feasibility of the CFD methods, as well as its capability for improving the design of the cooling systems.

References

[1] Bohn D, Heuer T. Conjugate flow and heat transfer calculation of a high pressure turbine nozzle guide vane. AIAA-2001-3304, 2001.
[2] Hylton L D, Mihelc M S, Turner E R, et al. Analytical and experimental evaluation of the heat transfer distribution over the surface of turbine vane. NASA-CR-168015, 1985.
[3] William D W, Leylek J H. Three-dimensional conjugate heat transfer simulation of an internally-cooled gas turbine vane. ASME GT2003-38551, 2003.
[4] Facchini B, Magi A, Scotti A, et al. Conjugate heat transfer simulation of a radially cooled gas turbine vane. ASME GT2004-54213, 2004.
[5] Dong P, Huang H Y, Feng G T. Conjugate heat transfer analysis of a high pressure turbine vane with radial internal cooling passages. Journal of Aerospace Power 2008; 23(2):201-207. [in Chinese]
[6] Bohn D, Kusterer K, Sugimoto T, et al. Conjugate analysis of a test configuration for a film-cooled blade under off-design conditions. ISABE-2003-1176, 2003.
[7] Kuserer K, Hagedom T, Bohn D, et al. Conjugate calculation for a film-cooled blade under different operation conditons. ASME GT2004-52719, 2004.
[8] Kuserer K, Hagedom T, Bohn D, et al. Improvement of a film-cooled blade by application of the conjugate calculation technique. ASME GT2005-68555, 2005.
[9] Heidmann J D, Kassab A J, Divo E A, et al. Conjugate heat transfer on a realistic film-cooled turbine vane. ASME GT2003-38553, 2003.
[10] Turner E R, Wilson M D, Hylton L D, et al. Analytical and experimental evaluation of surface heat transfer distributions with leading edge showerhead film cooling. NASA-CR-174827, 1985.
[11] Stainless Steel Technical Data. An Allegheny Technology Company, 2002.
[12] Menter F R, Langtry R B, Likki S R, et al. A correlation-based transition using local variables. Part I—model formulation. Journal of Turbomachinery 2006; 128(3): 413-422.
[13] Langtry R B, Menter F R, Likki S R, et al. A correlation-based transition using local variables part II—test cases and industrial application. Journal of Turbomachinery 2006; 128(3): 423-434.
[14] Li T M, Yan D C. Phenomenon of reverse transition on a heated flat plane with stable temperature stratification. Acta Scientiarum Naturalium Uuniversitatis Pekinensis 2005; 41(3): 381-387. [in Chinese]

Biographies:

Dong Ping Born in 1974, he received B.S. degree from Xi'an Jiaotong University in 1997 and M.S. degree from Harbin Institute of Technology in 2003, respectively. He now studies as a Ph.D. candidate in Harbin Institute of Technology. His main research interest is aerothermodynamics.
E-mail: dps777@163.com

Wang Qiang Born in 1982, he received B.S. and M.S. degrees from Harbin Institute of Technology in 2004 and 2006, respectively. He now studies as a Ph.D. candidate in the same school. His main research interest is aerothermodynamics.
E-mail: chuangwang.w@gmail.com

Guo Zhaoyuan Born in 1980, he received B.S. and M.S. degrees from Harbin Institute of Technology in 2003 and 2005, respectively. He now studies as a Ph.D. candidate in the same school. His main research interest is aerothermodynamics.
E-mail: guozhaoyuan@gmail.com